

# The self-assembly and evolution of homomeric protein complexes

Gabriel Villar,<sup>1</sup> Alex W. Wilber,<sup>1</sup> Alex J. Williamson,<sup>1</sup> Parvinder Thiara,<sup>1</sup> Jonathan P. K. Doye,<sup>1,\*</sup> Ard A. Louis,<sup>2</sup> Mara N. Jochum,<sup>1</sup> Anna C. F. Lewis,<sup>1</sup> and Emmanuel D. Levy<sup>3</sup>

<sup>1</sup>Physical and Theoretical Chemistry Laboratory, Department of Chemistry, University of Oxford, South Parks Road, Oxford, OX1 3QZ, United Kingdom

<sup>2</sup>Rudolf Peierls Centre for Theoretical Physics, University of Oxford, 1 Keble Road, Oxford, OX1 3NP, United Kingdom

<sup>3</sup>MRC Laboratory of Molecular Biology, Hills Road, Cambridge CB2 0QH, United Kingdom

(Dated: November 22, 2008)

We introduce a simple “patchy particle” model to study the thermodynamics and dynamics of self-assembly of homomeric protein complexes. Our calculations allow us to rationalize recent results for dihedral complexes. Namely, why evolution of such complexes naturally takes the system into a region of interaction space where (i) the evolutionarily newer interactions are weaker, (ii) subcomplexes involving the stronger interactions are observed to be thermodynamically stable on destabilization of the protein-protein interactions and (iii) the self-assembly dynamics are hierarchical with these same subcomplexes acting as kinetic intermediates.

PACS numbers: 87.15.km,87.14.ak,81.16.Dn,87.23.Kg

## INTRODUCTION

A large proportion of proteins are not monomeric *in vivo*, but instead 50-70% of those of known structure exist as homomeric protein complexes [1, 2]. These complexes are usually symmetrical with each protein in an identical environment [2]. This latter constraint limits the number of possible symmetries for such complexes. Thus, for homomeric tetramers, the two possible symmetries that obey this rule are cyclic ( $C_4$ ) or dihedral ( $D_2$ ) (Fig. 1). The  $C_4$  geometry involves only one type of interaction, whereas the  $D_2$  complex involves at least two self-complementary interactions. Interestingly, dihedral complexes are over ten times more abundant than cyclic complexes with the same number of subunits [3]. The origin of this preference seems to be evolutionary, namely because self-complementary interactions are easier to generate [4, 5] and because the evolution of dihedral complexes from a monomer does not have to proceed in a single step, e.g. a  $C_2$  dimer can be an intermediate on the evolutionary pathway to a  $D_2$  tetramer.

Insights into the evolution of homomeric protein complexes have recently come from a study that compared the complexes adopted by homologous proteins [3]. Although, for most homologues the quaternary structure is conserved, those cases where it is not conserved can tell us something about the evolutionary relationships between complexes of different symmetry. So, for example, it was found that where a tetramer shared an evolutionary relationship with a dimer, the tetramer always had  $D_2$  symmetry and in the majority of cases the dimer interface was conserved in the tetramer, supporting the postulated role of the dimer as an evolutionary intermediate. The study went on to show that the evolutionarily older interface was usually larger [3], and so presumably had a stronger interaction strength. In addition, mass

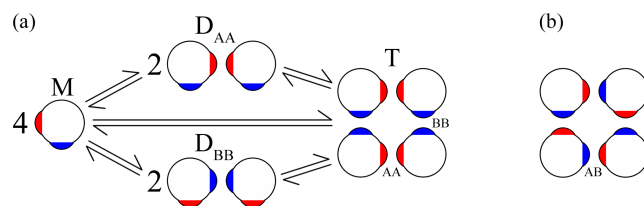


FIG. 1: (Colour Online) Schematic depiction of (a) a  $D_2$  tetramer and the possible equilibria involved in its formation, and (b) a  $C_4$  tetramer.

spectrometry revealed that when the disassembly of dihedral complexes was induced by changing the solution conditions (e.g. through the addition of denaturant) stable subcomplexes involving the larger interfaces were detected in the majority of cases [3]. Thus, the static structure of a dihedral complex, in particular the ratios of the interface areas, can provide insight into the evolution and assembly of the complex.

Here, we provide a framework for understanding these results for dihedral complexes by studying the thermodynamics and dynamics of assembly for a simple model of the complexes, particularly focussing on the role played by the relative strengths of the different interactions.

As the proteins in oligomeric complexes interact through highly specific contact surfaces or “patches”, we model the proteins using a patchy particle model used previously [6, 7], but with the introduction of an additional torsional component to the potential that ensures that the patches must not only point at each other to interact strongly, but also have the correct relative orientation. In this model, the repulsion between the particles is based upon an isotropic Lennard-Jones potential:

$$V_{LJ}(r) = 4\epsilon_{\text{ref}} \left[ \left( \frac{\sigma_{LJ}}{r} \right)^{12} - \left( \frac{\sigma_{LJ}}{r} \right)^6 \right], \quad (1)$$

but where the attraction is modulated by an orientational

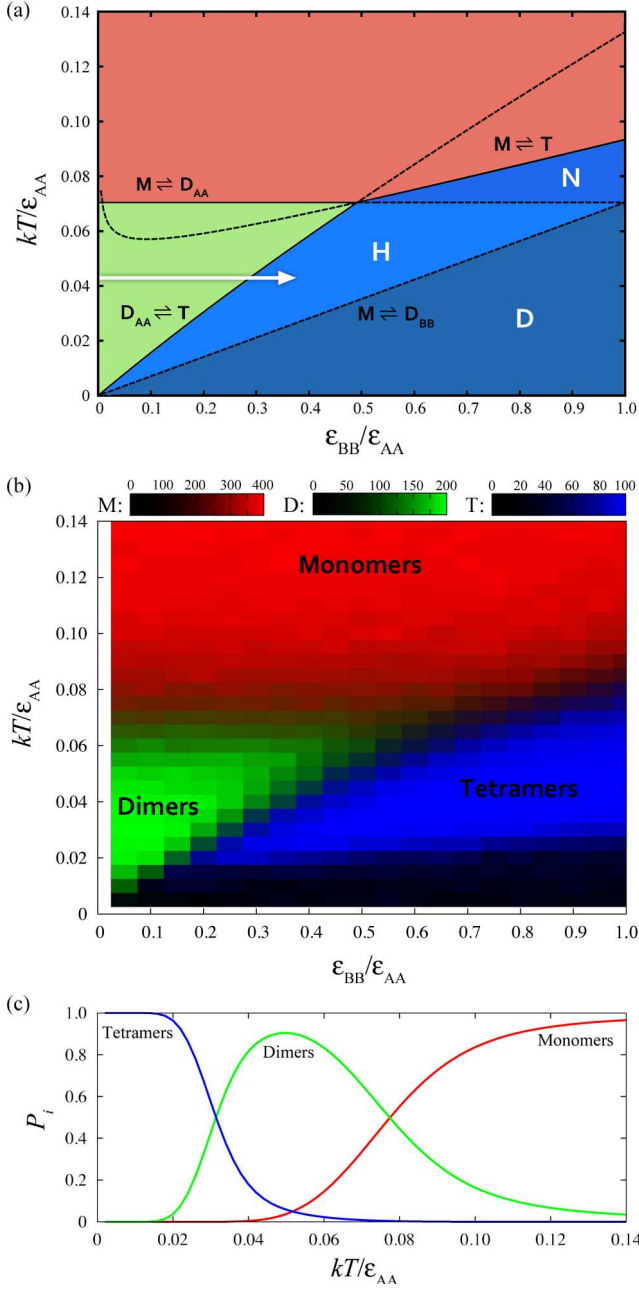


FIG. 2: (Colour Online) (a) Free-energy diagram showing the dependence of the most stable state of the  $D_2$  tetramer system on temperature and relative interaction strengths. The lines indicate where the equilibrium constants for the association reactions in Fig. 1(a) are one, and are solid when the equilibrium is between the two most stable forms, and dashed otherwise. The diagram is shaded according to whether monomers, dimers or tetramers are most stable. The arrow indicates a possible evolutionary path from a dimeric to a tetrameric complex. (b) Dependence of the final yields of monomers, dimers and tetramers from our dynamics simulations on  $kT/\epsilon_{AA}$  and  $\epsilon_{BB}/\epsilon_{AA}$ . Each pixel represents the result of a separate simulation, where each simulation started from a random configuration of the 400 particles and was  $10^8$  steps long. (c) Equilibrium probability of a particle being monomeric, or in a dimer or tetramer at  $\epsilon_{BB}/\epsilon_{AA} = 0.2$ .

term,  $V_{\text{ang}}$ . Thus, the complete potential is

$$V(\mathbf{r}_{ij}, \boldsymbol{\Omega}_i, \boldsymbol{\Omega}_j) = \begin{cases} V_{\text{LJ}}(r_{ij}) & r_{ij} < \sigma_{\text{LJ}} \\ V_{\text{LJ}}(r_{ij})V_{\text{ang}}(\hat{\mathbf{r}}_{ij}, \boldsymbol{\Omega}_i, \boldsymbol{\Omega}_j) & r_{ij} \geq \sigma_{\text{LJ}}, \end{cases} \quad (2)$$

where  $\boldsymbol{\Omega}_i$  is the orientation of particle  $i$ , and

$$V_{\text{ang}}(\hat{\mathbf{r}}_{ij}, \boldsymbol{\Omega}_i, \boldsymbol{\Omega}_j) = \max \left[ \frac{\epsilon_{\alpha\beta}}{\epsilon_{\text{ref}}} \exp\left(-\frac{\theta_{\alpha ij}^2}{2\sigma_{\text{pw}}^2}\right) \exp\left(-\frac{\theta_{\beta ji}^2}{2\sigma_{\text{pw}}^2}\right) \exp\left(-\frac{\phi^2}{2\sigma_{\text{tor}}^2}\right) \right] \quad (3)$$

where  $\theta_{\alpha ij}$  is the angle between the normal to patch  $\alpha$  on particle  $i$  and the interparticle vector  $\mathbf{r}_{ij}$ ,  $\phi$  is a torsional angle, and the ‘max’ selects the pair of patches that have the strongest interaction for the current geometry.  $\sigma_{\text{pw}}^{-1}$  and  $\sigma_{\text{tor}}^{-1}$  are measures of the specificity of the patch-patch interactions, and which we here choose to be the same for all patches [15]. By contrast, we allow the well-depth of the patch-patch interactions,  $\epsilon_{\alpha\beta}$  to vary ( $\epsilon_{\text{ref}} = \max[\epsilon_{\alpha\beta}]$ ). We also assume that interactions between pairs of patches not in contact in a complex to be zero (e.g.  $\epsilon_{AB} = 0$  for  $D_2$  tetramers).

To simulate the dynamics of our systems we use the ‘virtual move’ Monte Carlo algorithm of Whitelam and Geissler [8] as this generates the diffusional behaviour expected of particles and clusters in solution. To determine the thermodynamic properties of the system, we analytically calculate the partition functions for each state, as an ideal gas of clusters with rotational and vibrational degrees of freedom [16]. The vibrations are assumed to be harmonic and their frequencies are calculated by diagonalization of the Hessian.

We first consider the case of  $D_2$  tetramers, which for simplicity we choose to be planar. Fig. 2(a) shows the thermodynamics of the system as a function of the ratios of the interaction strengths  $\epsilon_{BB}/\epsilon_{AA}$ . Note, due to the symmetry we need only consider the case where  $\epsilon_{AA} > \epsilon_{BB}$ . At high temperature  $T$  (or equivalently low  $\epsilon_{AA}$ ) the system is monomeric. At  $\epsilon_{BB}/\epsilon_{AA} = 0$ , as the system is cooled, it passes from a ‘gas’ of monomers to a ‘gas’ of dimers. At non-zero  $\epsilon_{BB}/\epsilon_{AA}$  a transition from dimers to tetramers appears, and its transition temperature increases with  $\epsilon_{BB}/\epsilon_{AA}$  until a critical value of  $\epsilon_{BB}/\epsilon_{AA} \approx 0.5$  is reached beyond which dimers are no longer most stable for any value of  $kT/\epsilon_{AA}$  [17]. This critical value corresponds to the value of  $\epsilon_{BB}/\epsilon_{AA}$  at the ‘triple point’ where the three equilibrium lines in Fig. 2(a) meet.

This disappearance of the dimeric state is easy to understand. In the monomer to dimer transition the effective number of particles decreases by half, and the energy decreases by  $\epsilon_{AA}$ , whereas in the dimer to tetramer transition, although the number of clusters again decreases by half, the energy decreases by  $2\epsilon_{BB}$ . Therefore, the value of  $\epsilon_{BB}/\epsilon_{AA}$  for which the monomer to AA dimer

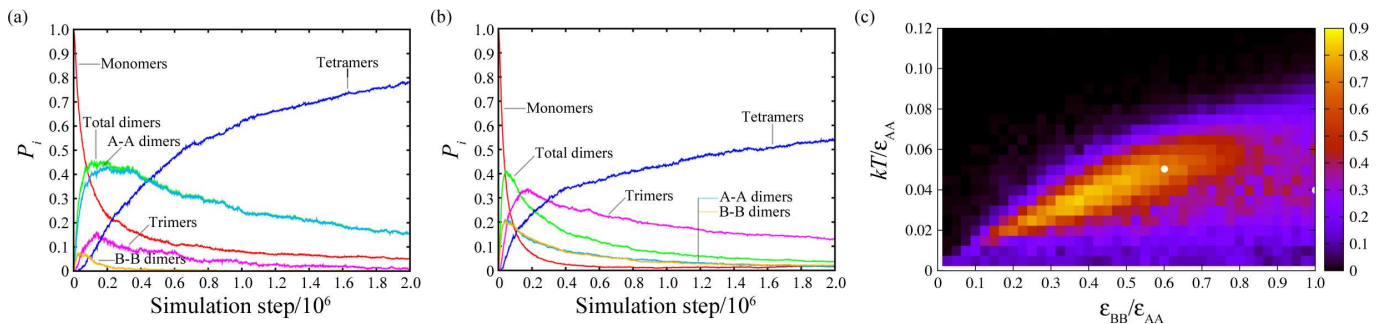


FIG. 3: (Colour Online) (a) and (b) Time dependence of the probability of a particle being in a particular state. For (a)  $\epsilon_{BB}/\epsilon_{AA} = 0.6$  and  $kT/\epsilon_{AA} = 0.05$  and (b)  $\epsilon_{BB}/\epsilon_{AA} = 1$  and  $kT/\epsilon_{AA} = 0.04$ . (c) Dependence of  $h$ , the hierarchicity index, on temperature and relative interaction strengths. The state points corresponding to (a) and (b) are marked by a white dot.

and the  $AA$  dimer to tetramer transitions occur at the same temperature is expected to be less than one, and is predicted to be 0.5, in agreement with Fig. 2(a), if the entropy change for both of these ‘dimerizations’ is simply assumed to be equal.

The reliability of our analytical thermodynamic model is confirmed by comparisons to results obtained using the Wang-Landau algorithm [9] and to our dynamics simulations. The kinetic yields of monomer, dimer and tetramer presented in Fig. 2(b) mirror the form of the free energy diagram (Fig. 2(a)), showing that near equilibrium is reached in the simulations except at very low temperatures where tetramers fail to form properly. In this latter case, the rate of cluster formation is so fast and the rate of cluster breakup so slow that all the monomers are used up before complete tetramers can form. Instead, many particles get trapped in trimers (e.g. Fig. 3(b)).

We can use Fig. 2(a) to help us understand the evolution of a  $D_2$  tetramer. The arrow in this figure shows a possible evolutionary pathways that takes the system from a dimeric state (i.e. where  $\epsilon_{BB}/\epsilon_{AA} = 0$ ) to a region of interaction space where tetramers are stable. The important thing to note is that the result of this evolution is a tetramer where the evolutionary newer  $BB$  interactions are weaker. This conclusion is in agreement with Levy *et al.*’s observation that newer patches have smaller areas [3], assuming that the interface area is a reasonable proxy for estimating the interaction strength.

We can also use Fig. 2(a) to consider the effect of additives that cause disassembly of protein complexes. If such additives destabilize all interactions equally, this process would correspond to a vertical pathway in Fig. 2(a). Therefore, if a complex has a value of  $\epsilon_{BB}/\epsilon_{AA} \lesssim 0.5$ , a thermodynamically stable dimeric phase will be seen for some concentration of the denaturant. The equilibrium probabilities of being in the different states along one such pathway is illustrated in Fig. 2(c). Again, as evolution will naturally take the system into a region to the left of the ‘triple point’, our results are in agreement with the mass spectroscopic results of Ref. 3 that de-

tected subcomplexes involving the stronger interactions, and with more traditional studies of tetramer formation [10, 11]. For example, Fig. 2(c) is very similar to results presented for phosphofructokinase [12].

Fig. 2(a) also allows us to think about the kinetic mechanisms of tetramer formation. In particular, the region in which tetramers are stable can be divided up into three subregions, depending on the stability of  $AA$  and  $BB$  dimers. In region  $N$  neither dimers are stable with respect to monomers, and so all intermediates are unstable and there will be a nucleation free energy barrier to tetramer formation. In region  $H$ ,  $AA$  dimers, but not  $BB$  dimers, are stable with respect to monomers, and so  $AA$  dimers will act as kinetic intermediates. In this region, we therefore expect a hierarchical self-assembly mechanism to dominate, in which  $AA$  dimers first form, and which in turn dimerize to form tetramers, rather than a mechanism which proceeds by sequential addition of monomers. Finally, in region  $D$  both  $AA$  and  $BB$  dimers are stable with respect to monomers and so all pathways for tetramer formation are downhill in free energy.

To test these predictions, we first look at the time dependence of the probabilities of being in the different states. In region  $D$ , the sequential passage from monomers to dimers to trimers to tetramers is evident (Fig. 3(a)). However, the initial rapid rise in the number of tetramers slows down as monomers become depleted, and the further formation of tetramers from trimers is dependent on cluster breakup (a relatively slow process) releasing additional monomers. By contrast, in region  $H$ ,  $AA$  dimers are clear intermediates and there is a steady growth of tetramers indicative of formation by dimer-dimer addition (Fig. 3(b)). Indeed, this plot has a very similar form to results for experimental studies on the rate of tetramer formation, such as for phosphoglycerate mutase [13] and lactate dehydrogenase [14].

We have further analysed how hierarchical the dynamics are by introducing a ‘hierarchicity’ index  $h$  that we define as the fraction of tetramer forming events that

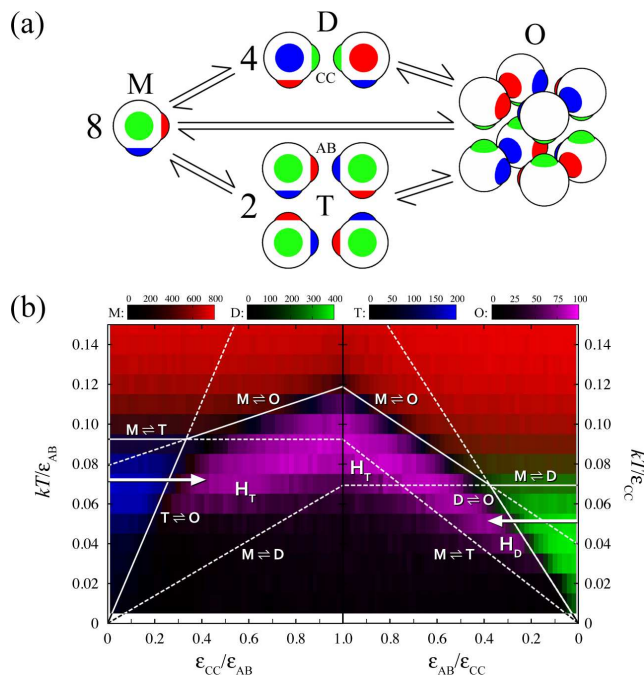


FIG. 4: (Colour Online) (a) Possible equilibria involved in the formation of a  $D_4$  octamer. (b) Free energy diagram showing the dependence of the most stable state on temperature and interaction strengths, superimposed on the final yields of monomers, dimers, tetramers and octamers in our dynamics simulations (800 particles,  $10^8$  steps). Note the change in the ordinate and abscissa in each half of the diagram.

occurred by dimer-dimer addition weighted by the fractional yield of tetramers. It can be clearly seen that the region in Fig. 3(c) where  $h$  is high corresponds well to region  $H$  in Fig. 2(a).

The approach we have put forward in this paper for understanding the formation of tetrameric complexes can be equally applied to complexes with other numbers of subunits. To illustrate this, we show the free energy diagram for the formation of a  $D_4$  octamer in Fig. 4(b) calculated by a simpler version of the theory used for Fig. 2(a), superimposed on the yields of different clusters obtained from our dynamics simulations. In our model for this system, the particles have three patches, two types of interaction (AB and CC) and for simplicity the octamer has a cubic shape (Fig. 4(a)). There are two possible hierarchical pathways for octamer assembly either via a  $C_4$  tetrameric intermediate that is stabilized by the AB interactions (region  $H_T$ ) or via dimers stabilized by the CC interactions (region  $H_D$ ), and this expectation is confirmed by analyses of the dynamics in these regions. In comparison to the results for the tetramer, it is noticeable that the low temperature region in which incomplete assembly leads to poor yields extends to higher temperature; this is a general trend for the self-assembly of more complex targets. The arrows in Fig. 4(b) illustrate potential evolutionary pathways of an octamer from a cyclic tetramer or a dimer, and which will again lead to com-

plexes where the newer patches are weaker and where the assembly is hierarchical.

In this paper we have shown how an analysis of the dependence of the thermodynamics and kinetics of homomeric protein complexes on the relative interaction strengths can provide a framework for understanding how their properties are constrained by their evolution, in particular their asymmetry in their interface areas and their hierarchical assembly. Although we have focussed on tetrameric complexes, the approach is easily generalizable to larger complexes and leads to similar conclusions. Thus, it would be very interesting if diagrams similar to the free energy diagrams of Figs. 2(a) and 4(b) could be mapped out experimentally by studying in detail how the thermodynamics of disassembly depends on the relative interface areas in a variety of protein complexes.

The authors are grateful for financial support from the EPSRC and the Royal Society.

\* Author for correspondence

- [1] E. D. Levy, J. B. Pereira-Leal, C. Chothia, and S. A. Teichmann, *PLoS Comput. Biol.* **2**, e155 (2006).
- [2] D. S. Goodsell and A. J. Olson, *Annu. Rev. Biophys. Biomol. Struct.* **29**, 105 (2000).
- [3] E. D. Levy, E. B. Erba, C. V. Robinson, and S. A. Teichmann, *Nature* **453**, 1262 (2008).
- [4] D. B. Lukatsky, K. B. Zeldovich, and E. I. Shakhnovich, *Phys. Rev. Lett.* **97**, 178101 (2006).
- [5] I. Andre, C. E. M. Strauss, D. B. Kaplan, P. Bradley, and D. Baker, *Proc. Natl. Acad. Sci. USA* **105**, 16148 (2008).
- [6] A. W. Wilber, J. P. K. Doye, A. A. Louis, E. G. Noya, M. A. Miller, and P. Wong, *J. Chem. Phys.* **127**, 085106 (2007).
- [7] J. P. K. Doye, A. A. Louis, I.-C. Lin, L. R. Allen, E. G. Noya, A. W. Wilber, H. C. Kok, and R. Lyus, *Phys. Chem. Chem. Phys.* **9**, 2197 (2007).
- [8] S. Whitelam and P. Geissler, *J. Chem. Phys.* **127**, 154101 (2007).
- [9] F. Wang and D. Landau, *Phys. Rev. Lett.* **86**, 2050 (2001).
- [10] R. Jaenicke and H. Lilie, *Adv. Protein Chem.* **53**, 329 (2000).
- [11] E. T. Powers and D. L. Powers, *Biophys. J.* **85**, 3587 (2003).
- [12] D. Deville-Bonne, G. Le Bras, W. Teschner, and J.-R. Garell, *Biochemistry* **318**, 1917 (1989).
- [13] R. Hermann, R. Rudolph, R. Jaenicke, N. C. Price, and A. Scobbie, *J. Biol. Chem.* **258**, 11014 (1983).
- [14] R. Hermann, R. Jaenicke, and G. Kretsch, *Naturwissenschaften* **70**, 517 (1983).
- [15] Throughout we use  $\sigma_{\text{tor}}/2 = \sigma_{\text{pw}} = 0.475$  and a number density of  $0.15 \sigma_{LJ}^{-3}$ . These values were chosen because they lead to efficient assembly of tetramers at  $\epsilon_{AA} = \epsilon_{BB}$ .
- [16] G. Villar *et al.*, in preparation.
- [17] The position of this critical value of  $\epsilon_{BB}/\epsilon_{AA}$  is insensitive to the potential parameters, being virtually constant as a function of density and patch specificity.